Atmos. Chem. Phys. Discuss., 12, 26685–26717, 2012
www.atmos-chem-phys-discuss.net/12/26685/2012/
doi:10.5194/acpd-12-26685-2012

Atmospheric Chemistry and Physics Discussions

Evaluation of a new middle-lower tropospheric CO_2 product using data assimilation

A. Tangborn[1,2], L. L. Strow[3], B. Imbiriba[4,*], L. Ott[1], and S. Pawson[1]

[1]Global Modeling and Assimilation Office, Goddard Space Flight Center, Greenbelt, MD, USA
[2]Joint Center for Earth Systems Technology, University of Maryland Baltimore County, Baltimore, MD, USA
[3]Dept of Physics, University of Maryland Baltimore County, Baltimore, MD, USA
[4]Núcleo de Meio Ambiente, Universidade Federal do Pará, Belém, PA, Brazil
[*]now at: Joint Center for Earth Systems Technology, University of Maryland Baltimore County, Baltimore, MD, USA

Received: 17 August 2012 – Accepted: 1 October 2012 – Published: 10 October 2012

Correspondence to: A. Tangborn (tangborn@umbc.edu)

Published by Copernicus Publications on behalf of the European Geosciences Union.

Abstract

Atmospheric CO_2 retrievals with peak sensitivity in the mid- to lower troposphere from the Atmospheric Infrared Sounder (AIRS) have been assimilated into the Global Modeling and Assimilation Office (GMAO) constituent assimilation system for the period 1 January 2005 to 31 December 2006. A corresponding model simulation, using identical initial conditions, circulation, and CO_2 boundary fluxes was also completed. The analyzed and simulated CO_2 fields are compared with surface measurements globally and aircraft measurements over North America. Surface level monthly mean CO_2 values show a marked improvement due to the assimilation in the Southern Hemisphere, while less consistent improvements are seen in the Northern Hemisphere. Mean differences with aircraft observations are reduced at all levels, with the largest decrease occurring in the mid-troposphere. The difference standard deviations are reduced slightly at all levels over the ocean, and all levels except the surface layer over land. These initial experiments indicate that the retrieved channel contains useful information on CO_2 in the middle to lower troposphere. However, the benefits of assimilating these data are reduced over the land surface, where concentrations are dominated by uncertain local fluxes and where the observation density is quite low. Away from these regions, the study demonstrates the power of the data assimilation technique for evaluating data that are not co-located, in that the improvements in mid-tropospheric CO_2 by the sparsely distributed partial-column retrievals are transported by the model to the fixed in-situ surface observation locations in more remote areas.

1 Introduction

A new atmospheric CO_2 product (UMBC AIRS CO_2) has been retrieved from the Atmospheric Infrared Sounder (AIRS) instrument on NASAs EOS-Aqua satellite (Imbiriba et al., 2012). This study uses the Goddard Earth Observing System, Version 5 (GEOS-5) atmospheric data assimilation system (DAS) to evaluate, in an integrated global

ACPD
12, 26685–26717, 2012

sense, the quality of these retrievals using a variety of independent, in-situ CO_2 measurements. The study also provides an assessment of how adequately this relatively sparse set of retrievals from AIRS, with at best several hundred observations per day, can be used to produce maps of the global CO_2 concentrations, which may eventually be used in "inverse" model applications to infer surface fluxes.

As described in Imbiriba et al. (2012), the UMBC AIRS CO_2 retrieval uses spectral radiance measurements from the emitted infrared wavelengths near 4.2 microns, leading to CO_2 partial columns that are weighted more strongly to the lower troposphere than retrievals from the 15-micron channels. These latter bands have been used in several other AIRS-based CO_2 retrievals, including the Jet Propulsion Laboratory (JPL) product (Chahine et al., 2008) and the European Centre for Medium-Range Weather Forecasts (ECMWF) product (Engelen et al., 2009), although the latter study included several channels at the shorter wavelengths. It also differs substantially from CO_2 products retrieved from the Greenhouse Gas Observing Satellite (GOSAT/Ibuki) satellite (e.g. Yokota et al., 2009) that are based on reflected solar radiance measurements near 2 microns.

The UMBC AIRS CO_2 retrievals are performed at observation locations chosen using a stringent quality control process that restricts data to cloud-free, uncontaminated scenes (Strow and Hannon, 2008). The sparseness of these data and their global distribution, often over oceans, precludes the use of vicarious calibration exercises in their evaluation. By transforming the partial columns derived from the time series of AIRS data to global atmospheric concentration maps, the DAS provides a framework for evaluating the retrievals using existing CO_2 observations. While this approach does not replace the need for targeted evaluation efforts, it does provide an alternate methodology that uses existing observation networks. In this case, the DAS provides the observation operators (and their inverses) that map between the partial columns at the observation locations and atmospheric concentrations on a specified grid, and the transport computations that effectively interpolate from the AIRS observation locations

ACPD
12, 26685–26717, 2012

to the sparse locations of the in-situ observations. The observations used for evaluation are local CO_2 concentrations at the surface and on aircraft flight tracks.

An additional benefit of the DAS is that the resultant maps of CO_2 concentrations are valuable resources for helping to understand the spatial-temporal structure of regional CO_2 distributions and assessing their consistency with surface fluxes. This study includes a comparison of a model simulation with the assimilated CO_2 data. Apart from the data constraint in the assimilation, the two products are derived using an identical system (initial states, transport, and surface fluxes), so that differences between the model and the assimilation can be attributed to the innovations computed by the DAS. These differences are a central part of the evaluation but they are also used to help evaluate the realism of the surface flux distributions applied in the system. This puts the atmospheric DAS used in this work in the context of inverse model studies, in which new estimates of surface fluxes are computed as a part of the optimization (e.g. Chevallier et al., 2009; Baker et al., 2010; Feng et al., 2011).

The rest of the paper is organized as follows: the AIRS 4 µm retrievals are described in Sect. 2, followed by some background on the model and assimilation system in Sect. 3; the assimilation results and verification with in-situ data are presented in Sect. 4, and the discussion is given in Sect. 5.

2 The AIRS CO_2 retrievals used in this work

The Atmospheric Infrared Sounder on NASA's Aqua satellite measures infrared radiances in the wavelength range 3.7 to 15.4 microns with 2378 channels. A number of these channels are sensitive to CO_2, including several around 15 µm which have peak sensitivity between 150 and 400 hPa (Chahine et al., 2008). Examples of the 15 µm averaging kernels are shown in Fig. 1a. The peak sensitivity is generally higher in the tropics, and there is essentially no sensitivity below 700 mb. Given that one focus of atmospheric carbon cycle research is on improving estimates of surface fluxes, retrievals from channels with sensitivity lower in the troposphere are desirable.

ACPD
12, 26685–26717, 2012

In this work we use a cluster of channels in the 4 µm region (2400 cm^{-1}) which have peak sensitivity around 450 hPa (Imbiriba et al., 2012). The actual channels used are, long wave CO_2: 790.229, 791.649 cm^{-1} and shortwave CO_2: 2388.87, 2389.84, 2390.82, 2391.80, 2415.56, 2416.56, 2417.56, 2418.56 cm^{-1}. Two of these channels were also used by Engelen et al. (2009), while the remaining have not been used in any CO_2 retrieval or assimilation. These channels were chosen for their sensitivity to CO_2 in the middle to lower troposphere, as shown by the averaging kernel in Fig. 1b. The ten channels include five pairs in which one channel is not sensitive to CO_2 and the other one is, which enables the CO_2 impacts to be separated from atmospheric and surface effects on radiances. Using a cluster of channels reduces the statistical noise to 4.8 ppm per reported observation. The atmospheric state, including temperature profiles, are provided by the ECMWF analyses which are interpolated in time and space to the precise AIRS observation event. In February 2006 there was a major change in the ECMWF system largely affecting the simulated temperature profiles and hence changing the bias in our retrieved CO_2 with respect to in situ measurements. In order to properly take this shift into account, the data needed to be recalibrated after this date. This one-time effect was treated with a single bias reduction of 2 ppm.

The retrievals used are restricted to clear sky observations only, which reduces the total observation count to a relatively small fraction of the AIRS measurements. In fact, there can be as many as four to five successive days in which there are no observations that pass through the cloud screen. The remaining observations are then superobbed to the model grid size (2° × 2.5°). Figure 2 shows the observation counts for the superobbed data for the period January–February 2005. There are relatively few observations over continental regions, particularly North America and Asia, with a relatively greater number over oceans. The retrievals, done without an a priori, result in a mid-to-lower tropospheric CO_2 mixing ratio with associated averaging kernels. A typical averaging kernels (Fig. 1b) show that the sensitivity at 700 hPa is still more than 1/3 of the peak level.

ACPD
12, 26685–26717, 2012

3 Transport model and assimilation system

The CO_2 assimilation module was originally developed for ozone (Stajner et al., 2001, 2008) and later adapted for CO (Tangborn et al., 2009). The algorithm is the Physical-space Statistical Analysis System (PSAS) (Cohn et al., 1998), in which the standard 3DVAR is reformulated and solved in observation space. Thus the solution vector, solved by conjugate gradient methods, is the same length as the observation vector. This is a particularly efficient and attractive approach when assimilating relatively sparse observation sets, such as observations from a single satellite.

The current application of this system to AIRS CO_2 retrievals involves the introduction of the AIRS forward operator which consists of the following steps: interpolate the 72 model levels to the 101 averaging kernel pressure levels, $\mathbf{H}_{\mathrm{I}}$ (101 × 72 matrix); multiply the 101 CO_2 values by the appropriate averaging kernel values, summing over all levels and divide by the sum of the averaging kernel, $\mathbf{H}_{\mathrm{ak}}$ (1 × 101 matrix); thus the entire forward operator is $H = \mathbf{H}_{\mathrm{ak}}\mathbf{H}_{\mathrm{I}}$. The PSAS algorithm solves the innovation equation

$$(HP^{\mathrm{f}}H^{T} + R)\boldsymbol{y} = \left(c^{\mathrm{o}}_{\mathrm{ca}} - \mathcal{H}(x^{\mathrm{f}})\right) \tag{1}$$

for the vector $\boldsymbol{y}$, in observation space. Note that the length of $\boldsymbol{y}$ is equal to the number of observations. The linearization of the observation operator, $\mathcal{H}$, is H, and error statistics are represented by the forecast error covariance, P^{f}. The observation error covariance, R is a diagonal matrix made up of observation error variances, which means that the observation errors are assumed to be spatially uncorrelated. The observations, $c^{\mathrm{o}}_{\mathrm{ca}}$, are column averaged using the averaging kernel with units of ppm.

The solution is then transformed to model space via

$$x^{\mathrm{a}} - x^{\mathrm{f}} = P^{\mathrm{f}}H^{T}\boldsymbol{y} \tag{2}$$

to obtain the analysis increment $x^{\mathrm{a}} - x^{\mathrm{f}}$, where x^{a} is the CO_2 analysis and x^{f} is the CO_2 forecast.

ACPD
12, 26685–26717, 2012

The forecast error covariance, P^f, is specified using a separable and non-isotropic error covariance model in which the error standard deviation, σ^f, is set as a constant percentage of the local CO_2 mixing ratio ($\sigma^f = \alpha x^f$) and the horizontal error correlation is a function of latitude. This results in a state dependent error covariance because the error standard deviation satisfies the constituent advection equation. Further adjustments to background errors are needed to account for the larger errors occurring in the Northern Hemisphere, which is discussed below. We have chosen to restrict corrections to the troposphere where CO_2 errors are generally larger than in the stratosphere. This is done by reducing the background error standard deviation in the stratosphere by a factor of 10.

Tuning runs were done in which the background standard deviation is varied using the standard deviation parameter α. Comparisons were then made with several ground and aircraft based in situ CO_2 data sets. These include measurements from the CCGG (Carbon Cycle Greenhouse Gases) Cooperative Air Sampling Network (Conway et al., 2011), NOAA GMD Vertical Profile Carbon Cycle Network (aircraft data) and the Intercontinental Chemical Transport Experiment-Phase B (INTEX-B) (Singh et al., 2009). Initial testing showed that that a single value of α for the entire atmosphere is not sufficient because errors in the Northern Hemisphere are considerably higher than those in the Southern Hemisphere. This is even though the background error model results in larger errors where CO_2 is higher, the comparisons with in situ data indicate that the error increase is even larger and tends to increase through the northern mid-latitudes. This increase is likely due to the larger variability (and therefore uncertainty) of CO_2 over continental land masses. Thus we use a factor α that depends on latitude. The optimal values of α from these tuning runs were found to be:

$\alpha = 0.001$ for latitude $< 0°$

$\alpha = 0.004$ for $0 \leq$ latitude $< 25°$ N

$\alpha = 0.008$ for latitude $\geq 25°$ N.

ACPD
12, 26685–26717, 2012

These values of α results in surface background error standard deviations which vary from around 3 ppm in the northern mid-latitudes to about 0.35 ppm near the South Pole. The background error correlation length used in the assimilation also varies with latitude and direction.

This background error covariance model differs from previous AIRS CO_2 assimilation studies. Engelen et al. (2009) employed the NMC method (Parrish and Derber, 1992) which uses statistics from 24 and 48 h forecasts. This approach tends to underestimate errors where there are no observations, and they compensate for this by a factor of 8 inflation factor at the surface. But a constant inflation will not give the largest errors where flux estimate errors are the largest. Ensemble Kalman filter methodology shows great potential for estimating background errors (Liu et al., 2012), but this still does not address model errors as directly as comparison with in situ observations.

The CO_2 forecast fields, x^f, used by the assimilation are produced by the GEOS-5 Atmospheric General Circulation Model (AGCM), (Rienecker et al., 2008) using analyzed meteorology from the Modern-Era Retrospective Analysis for Research and Applications (MERRA; Rienecker et al., 2011). Surface fluxes of CO_2 are prescribed for fossil fuel, ocean, and biosphere fluxes derived from the TransCom-3 protocol (Gurney et al., 2002) and biomass burning emissions from the Global Fire Emissions Database, Version 2 (GFED-2; van der Werf et al., 2006). For this study, the model is run using a 2° latitude by 2.5° longitude horizontal resolution with 72 layers between the surface and 0.1 hPa.

4 Results

We have carried out a two year assimilation experiment for the period 1 January 2005 to 31 December 2006. A model simulation using identical initial states, meteorological fields and CO_2 boundary fluxes was also performed. Comparisons of the assimilated and simulated CO_2 distributions allows the impact of the assimilation to be examined.

ACPD
12, 26685–26717, 2012

A typical analysis increment ($x^f - x^a$) at a latitude of 135° W is shown in Fig. 3. The rapid decay above 300 hPa is due to the reduced background errors in the stratosphere and impact extends well into the lower troposphere. The shape of the increment depends on both the local averaging kernel and the local background error covariance.

Monthly mean CO_2 values at six CCGG surface flask sites are shown in Fig. 4, along with assimilated and simulated CO_2 fields, interpolated to the observation locations. Over the first few months, the assimilated (red curve) CO_2 diverge from the modeled (blue) fields, generally moving closer to the observations (black), indicating a spin up time for the assimilation of about 6 months. This long period for the assimilation system to respond is most likely due to the small number of observations. In the Southern Hemisphere (a, b), where there is little seasonal cycle in CO_2, the improvements due to the assimilation are particularly important because the initial difference between the model and observations is only about 1 ppm. In the Northern Hemisphere (c, d), the seasonal cycle is reproduced accurately in the model, but with a bias of 2–4 ppm. The assimilation reduces the bias, but does not significantly change the seasonal cycle. The flask site at 40° N (BAO) is the least successful, but still shows some reduction in the difference with measured values. Finally, in the northern high latitudes (f, g) where the is a strong seasonal cycle is fairly well captured by the model. The assimilation reduces the bias, but it is not clear if there is a significant improvement to the annual cycle.

In order to get a more quantitative picture of how the assimilation is affecting the accuracy of the surface layer CO_2, we plot the mean and standard deviations of the difference between measurements and model or analyses (usually called observation minus model or analysis, $O - M$ or $O - A$) at the eight CCGG sites in Fig. 5. The mean differences (a) show a consistent decrease in the bias when the AIRS retrievals are assimilated. This decrease is particularly noteworthy in the Southern Hemisphere, where the declines are all more than 50 %. On the other hand, the standard deviation of the differences (b) show generally small increases. This indicates that the assimilation is not helping to improve estimates of annual variability at these surface locations, in spite

ACPD
12, 26685–26717, 2012

of the decrease in the bias. The lack of improvement in the random error at the surface most likely has two causes: the first is that this AIRS channel has peak sensitivity to CO_2 in the mid-troposphere, and essentially none inside the boundary layer. Thus any improvements that are made at the surface can only happen through corrections to CO_2 aloft that are transported to the surface by the model. We will discuss this process later in this section. The second cause is the sparsity of the clear sky AIRS observations. Figure 2 shows that there are many days when no observations are available, and sometimes none for several days at a time. This should impact the random error component to a greater degree because alternating between forcing the CO_2 field with observations and then allowing it to relax back towards the model state would likely add non-physical temporal variations into the field. Also, the long spin-up time for the assimilation (around 6 months) means that the assimilation cannot improve estimates for rapidly changing seasonal variations. This would be particularly true at the surface where there is no direct impact of the observations. We discuss the impact of the sparse data further in this section.

There are a number of sources of in situ measurements from aircraft, and we have used two of these for assessing the impact of the assimilation. The locations of these flights during the assimilation period are shown in Fig. 6. In Figs. 7 and 8 we plot the mean and standard deviation of the differences between the two model runs and NOAA/ESRL aircraft data for 3 altitude ranges. Except for one exception (HAA, Hawaii), all of these measurements are made over continental North America where there are relatively few observations. The mean differences show that the biggest improvements come in the mid-troposphere (b), while the surface (a) and upper troposphere (c) show somewhat mixed results, with slightly more than half the sites showing reduced differences with assimilation. This is consistent with the peak sensitivity of the retrieved AIRS channels at around 500 hPa. The standard deviations shown in Fig. 8 indicate very small changes due to the assimilation. At the surface (a), there are slightly more locations that show increases; while in the mid-troposphere (b), every location shows

ACPD
12, 26685–26717, 2012

a modest decrease. In the upper troposphere (c), the very small changes are mainly downward.

The INTEX-B campaign carried out during January–May 2006, consisted of numerous flights across the Central and Western United States, as well as excursions over the Pacific Ocean (Fig. 6b). So while there may be some overlap with the NOAA aircraft data, the main difference is that the flights are not done at discrete locations and involve travel over larger distances. In addition, the data available for comparison is far greater due to the frequent sampling. We have divided the data into observations taken over the Pacific ocean (a, b) and over North America (c, d), and mean and standard deviation differences (forecast–observation) in Fig. 9. Over the Pacific, the mean and standard deviation differences between the model and INTEX are smallest near the surface and increase with altitude, and they are reduced at all levels by the assimilation. This can be attributed to the small surface fluxes which means that most of the CO_2 is transported over the ocean at higher levels. Over North America the differences are generally smaller at higher altitudes, particularly in the standard deviation, indicating that flux misspecification is the primary source of errors. While the mean differences are reduced by the assimilation at all levels, the standard deviation is only consistently reduced above 3000 m. The difference between the comparisons over the Pacific and North America are the result of larger fluxes (and therefore larger flux errors) and the smaller number of observations over land.

These results have some discrepancies with the NOAA aircraft comparisons. Most notable is the magnitude of both the mean and standard deviation differences over North America are smaller for INTEX-B than for NOAA aircraft data. This can be explained in part by the different regions of North America where data was collected, and probably is an indication that errors are not very uniform due to the higher variability. This can also been seen in the variability of the standard deviation differences with NOAA aircraft data, which range from 2 to 7 ppm.

The improvement in the mean CO_2 fields at the surface that result from assimilating AIRS retrievals give some hope (but certainly does not guarantee) that these channels

ACPD
12, 26685–26717, 2012

may be useful for CO_2 flux inversion, particularly when combined with other data sets. Baker et al. (2006) pointed out that in the tropics, model errors in vertical mixing tend to dominate, making it difficult to obtain an accurate estimate of CO_2 profiles. It would therefore be valuable to have additional tropospheric information of CO_2 with different vertical weightings. But the results above raise the questions as to how the assimilation of this data improves the mean comparisons in the surface layer, given that the peak sensitivity is around 500 hPa, with very little sensitivity at the surface. The most likely answer is that the assimilation makes corrections centered in the 400 to 600 hPa range (about 4000 to 7000 m), which are then then transported to the surface through convection in the model.

We investigate how improvements in mean CO_2 at the surface might take place by following the analysis increment from Fig. 3 during the first 24 h after assimilation. Figure 10 shows the difference between the assimilation run and the free model model run CO_2 in a vertical slice that follows the location of the maximum difference as it moves eastward. The difference between the two runs will consist of much more than one increment, and will also include differences from past observations. Nevertheless, this series of snapshots shows the clear evolution of a particular increment in the atmosphere (the data sparseness is an advantage for this analysis). In panel (a) the initial negative difference can be see near 64° N and 135° W, which is the result of an observation assimilated at 0Z. The impact of the observation is maximum between 700 and 400 hPa. This structure is due to a combination of the averaging kernel, which peaks near 500 hPa, the background error variance (proportional to the local CO_2 mixing ratio) which is generally larger lower in the atmosphere, and the vertical error correlation. After 12 h (b), the peak difference has moved eastward and the difference at the surface has increased due to model transport. After 24 h (c), it is clear that though the increment is decaying (through atmospheric dispersion and mixing), it continues to have an impact at the surface as it moves eastward. These snapshots show how an observation in one region can impact the CO_2 field nearby, and how the mid-tropospheric sensitivity

ACPD
12, 26685–26717, 2012

can translate into improvements at the surface. This is one possible explanation for the surface layer improvements shown in Fig. 4.

The contrast between the comparisons with NOAA/ESRL and INTEX-B aircraft measurements also needs further investigation. The mean differences between the assimilation and INTEX-B is between 0.5 and 1.0 ppm (even over North America), while the difference with NOAA/ESRL aircraft data varies from 0.5 to about 3.5 ppm. The disparity in the standard deviation differences is even more pronounced, 1 to 4 ppm compared with INTEX-B and 2 to 8 ppm compared with NOAA/ESRL. The INTEX-B measurements made over the Eastern Pacific have lowest errors, while most of the NOAA/ESRL measurements are made over North America, where there are far fewer UMBC AIRS observations. These differences can be better understood by plotting monthly mean differences between the assimilation and free model run at 40° N, which is near many of the aircraft measurements. These differences, for the period March–August 2005, are shown in Fig. 11. Generally we see that the region over North America (about 120° W to 60° W) is changed much less than the adjacent ocean regions. For example, in March 2005 over the Eastern Pacific (west of 120° W), changes the CO_2 field are largest at the surface, while the change over North America are largest above 500 mb. Rarely do the mean changes reach all the way to the surface over North America. The surface layer can have a correction in the opposite direction from the free troposphere (e.g. July 2006). This is likely due to both the limited continental UMBC AIRS retrievals and the larger fluxes on land, combined with corrections transported from other regions.

We can use these comparisons to understand the mean and standard deviation differences with the NOAA/ESRL aircraft data. Figure 12 shows the NOAA/ESRL CO_2 profiles (black line) at the Trinidad Head Observatory (THD) at (124° W, 41° N) along with the free model run (blue) and assimilation (red), interpolated to the profile locations. The profiles shown are monthly averages for the period March–August 2005. In March (Fig. 12a), the analysis profile is very close to the aircraft profile, but does not achieve the same vertical structure. During this time, Fig. 11a shows a large downward correction to CO_2 at all levels. During the months April and May, there are very few

ACPD
12, 26685–26717, 2012

observations and therefore very little correction at the profile location (Fig. 11c, d). This results in assimilation profiles that have moved back towards the free running model profile during these two months. In the last three panels (d–f) both the assimilation and free running model begin to capture the vertical structure more accurately. During this time there are still relatively few observations near THD, so that improvements come from better vertical representation in the model. This is particularly apparent in June 2005 (Fig. 12d), where the vertical gradient is very accurately represented, with a bias of about 1 ppm in the assimilation and 3 ppm in the model.

The temporal variations in the profile at THD can also help to explain the error standard deviation differences with aircraft data. The analysis profile is seen to oscillate between the aircraft measurements (Fig. 12a), and the free running model profile (Fig. 12c). This type of movement causes an overall increase in the standard deviation difference with aircraft data, and is caused by the limited availability of retrievals over land. This contrasts with the consistently large decreases in error standard deviation differences with the INTEX-B aircraft data over the Eastern Pacific for the assimilation, where a much larger number of retrievals are available.

Larger scale changes in CO_2 due to the assimilation of AIRS retrievals can be examined by calculating the total column (XCO_2) over North America for both the free model and the assimilation runs. Figure 13 shows the a comparison of the season cycle of column CO_2 over North America computed from July, 2005 through June 2006 using the model and assimilation fields. The effect of the assimilation is to slightly reduce the magnitude of the seasonal cycle in column CO_2 from a 5.3 ppmv peak-to-trough amplitude in the model compared to a 4.5 ppmv amplitude when AIRS data are assimilated. The greatest differences occur in August–September and February–March. Because the seasonal cycle in simulated CO_2 over North America is governed primarily by the prescribed biosphere fluxes, the results may indicate that AIRS data are useful in assessing flux errors. The changes to the seasonal cycle found here are probably smaller than would be obtained using a less sparse set of retrievals. It should be noted

ACPD
12, 26685–26717, 2012

that these results include a single year of simulation; future work will consider a longer timer period to examine the impact of AIRS data over longer timescales.

5 Summary and discussion

A new atmospheric CO_2 partial-column dataset, derived from a cluster of AIRS spectral radiance channels mainly near 4 µm, with peak sensitivity to CO_2 variations in the middle troposphere (Imbiriba et al., 2012), has been assimilated into GEOS-5. The stringent clear-sky criterion placed on these retrievals means that, at best, several hundred observations are available each day. The assimilation ran through 2005 and 2006. There are both positive and negative aspects of these results, which are discussed here.

One of the most positive aspects of this work is the generally beneficial impact of CO_2 data assimilation on the concentration distributions, even when using a model that uses incorrect source-sink distributions. The impacts of the assimilation are assessed using in-situ measurements and comparing the assimilated distributions with those from an otherwise identical free-running model. Evaluation using surface flask observations reveals that, compared with a simulation, the assimilation of the AIRS mid-tropospheric CO_2 retrievals improves the annual cycle in surface concentrations, especially in the Southern Hemisphere. Comparison with aircraft observations shows different impacts over land and oceans. Over North America, where NOAA aircraft observations are routinely made, the assimilation leads to improvements in CO_2 near 500 hPa, with only a small benefit near the surface. Over the Pacific, comparison with aircraft observations from the Intex-B field mission reveals larger positive impacts near the surface than over land. In the Southern Hemisphere and over oceans in the Northern Hemisphere, where local CO_2 fluxes are weak and where more observations are available to assimilate, the assimilation leads to substantial reductions in the mean bias compared to in situ observations. The standard deviation differences are not consistently reduced, but generally remain below 1 ppm in these regions.

ACPD
12, 26685–26717, 2012

The CO_2 fluxes used in this work are not state of the art: for instance, the land biosphere fluxes from Transcom (Gurney et al., 2002; Baker et al., 2006) were derived using a Bayesian inversion technique constrained with surface CO_2 concentrations from many years in suite of transport models, each of which used winds from a single year; the biomass-burning emissions from GFED2 have been updated (GFED3). The mismatch between these imposed fluxes and the true ones (for the time and location of the assimilation) lead to atmospheric concentrations that depart substantially from the direct observations over North America. The strength of the fluxes, coupled with the absence of near-surface information content of these retrievals, means that the assimilation does not substantially improve the bias in CO_2 concentrations in this region. This means that more representative CO_2 fluxes need to be used in regions where they are large. However, regional maps of land biosphere CO_2 fluxes are known to have large uncertainties (e.g. Jung et al., 2011), meaning that they result in large biases in the background state in the data assimilation system. Inverse approaches, that include the flux as a component of the state vector in the assimilation, offer the advantage of continuously correcting surface fluxes along with the atmospheric concentrations, but to date these also result in significant uncertainties (e.g. Baker et al., 2010; Feng et al., 2011; Nassar et al., 2011).

Compared to the work of Engelen et al. (2009), the data assimilation in this work results in a much larger improvement in the systematic and random components of differences from in-situ observations (compared to the equivalent model). There are several potential reasons for this, including the stringent cloud screening used in the UMBC AIRS CO_2 retrievals and differences in background error covariance modeling. The state dependent model used here accounts for variability due to the CO_2 field itself and is adjusted using comparisons with ground based observations. The NMC method used by Engelen is unlikely to account for the large variations in errors that typically occur in flux models. In a more recent work, Liu et al. (2012), assimilated CO_2 retrievals using channels near 15 µm and showed positive mean comparisons with in situ observations at all levels of the atmosphere. Much of this improvement can possibly be

ACPD
12, 26685–26717, 2012

attributed to the use of the Local Transform Ensemble Kalman Filter (LETKF), which provides background error covariance estimates that reflect uncertainties in the meteorological fields. However, at some of the comparison locations (e.g. HFM), the free running model has a very large bias compared to the observations, so that improvements due to assimilation are relatively easy to achieve. It is likely that a hybrid approach that includes both ensemble error estimation and error statistics generated through comparisons with ground and aircraft based observations. This combination can account for errors that originate in both the transport and surface fluxes.

These results suggest that the UMBC AIRS CO_2 product is beneficial for constraining global atmospheric concentrations, despite the sparse spatial coverage. The version of the product used in this work was derived using meteorological fields from ECMWF, then assimilated into GEOS-5. A more robust long-term approach will investigate using GEOS-5 fields for all aspects of the work, including the possibility of cycling the retrievals through the assimilation system. This would allow use of GEOS-5 predictions of CO_2 as prior states in the retrieval, and also allow exploitation of consistent land-surface analyses that are being developed (e.g. Reichle et al., 2011).

Another aspect of this work that can be further exploited is the cross-calibration of different observations. For instance, extending the period of study to 2010–2011 will allow tests of the consistency between these NIR retrievals from AIRS with the reflected solar infrared measurements made by GOSAT (Yokota et al., 2009). Ultimately, the joint assimilation of CO_2 measurements from AIRS, GOSAT and other platforms is a highly desirable focus that should lead to better understanding of the atmospheric carbon balance.

Acknowledgements. The authors wish to thank Thomas Conway and Pieter Tans for the use of NOAA/ESRL CCG flask data, and Colm Sweeney for the NOAA GMD Carbon Cycle Vertical Profile Network, and the INTEX-B team for access to this data set. Computations were performed using the high-end computers at the NASA Center for Climate Simulation (NCCS).

ACPD
12, 26685–26717, 2012

References

Baker, D. F., Law, R. M., Gurney, K. R., Rayner, P., Peylin, P., Denning, A. S., Bousquet, P., Bruhwiler, L., Chen, Y.-H., Ciasis, P., Fung, I. Y., Heimann, M., John, J., Maki, T., Maksyutov, S., Masarie, K., Prather, M., Pak, B., Taguchi, S., and Zhu, Z.: TransCom 3 inversion intercomparison: impact of transport model errors on the interannual variability of regional CO_2 fluxes, 1988–2003, Global Biogeochem. Cy., 20, GB1002, doi:10.1029/2004GB002439, 2006.

Baker, D. F., Bösch, H., Doney, S. C., O'Brien, D., and Schimel, D. S.: Carbon source/sink information provided by column CO_2 measurements from the Orbiting Carbon Observatory, Atmos. Chem. Phys., 10, 4145–4165, doi:10.5194/acp-10-4145-2010, 2010.

Chahine, M. T., Chen, L., Dimotakis, P., Jian, X., Li, Q., Olsen, E. T., Pagano, T., Randerson, J., and Yung, Y. L.: Satellite remote sounding of mid-tropospheric CO_2, Geophys. Res. Lett., 35, L17807, doi:10.1029/2008GL035022, 2008.

Chevallier, F., Engelen, R. J., Carouge, C., Conway, T. J., Peylin, P., Pickett-Heaps, C., Ramonet, M., Rayner, P. J., and Xueref-Remy, I.: AIRS-based versus flask-based estimation of carbon surface fluxes, J. Geophys. Res., 114, D20303, doi:10.1029/2009JD012311, 2009.

Conway, T. J., Lang, P. M., and Masarie, K. A.: Atmospheric carbon dioxide dry air mole fractions from the NOAA ESRL Carbon Cycle Cooperative Global Air Sampling Network, 1968–2010, Version: 2011-10-14, available at: ftp://ftp.cmdl.noaa.gov/ccg/co2/flask/event/ (last access: October 2012), 2011.

Engelen, R. J., Serrar, S., and Chevallier, F.: Four-dimensional data assimilation of atmospheric CO_2 using AIRS observations, J. Geophys. Res., 114, D03303, doi:10.1029/2008JD010739, 2009.

Feng, L., Palmer, P. I., Yang, Y., Yantosca, R. M., Kawa, S. R., Paris, J.-D., Matsueda, H., and Machida, T.: Evaluating a 3-D transport model of atmospheric CO_2 using ground-based, aircraft, and space-borne data, Atmos. Chem. Phys., 11, 2789–2803, doi:10.5194/acp-11-2789-2011, 2011.

Gurney, K. R., Law, R. M, Denning, A. S., Rayner, P. J., Baker, D., Bousquet, P., Bruhwiler, L., Chen, Y. H., Ciais, P., Fan, S., Fung, I. Y.;, Gloor, M., Heimann, M., Higuchi, K., John, J., Maki, T.;, Maksyutov, S., Masarie, K., Peylin, P., Prather, M., Pak, B. C., Randerson, J., Sarmiento, J., Taguchi, S., Takahashi, T., and Yuen, C. W.: Towards robust regional estimates of CO_2 sources and sinks using atmospheric transport models, Nature, 415, 626–630, 2002.

ACPD
12, 26685–26717, 2012

Imbiriba, B., Strow, L., Hannon, S., Schon, P., Powers, L., and de Souza-Machado, S.: Atmospheric model issues on local measurement of CO_2 using the Atmospheric Infrared Sounder (AIRS), in preparation, 2012.

Jung, M., Reichstein, M., Margolis, H. A., Cescatti, A., Richardson, A. D., Arain, M. A., Arneth, A., Bernhofer, C., Bonal, D., Chen, J. Q., Gianelle, D., Gobron, N., Kiely, G., Kutsch, W., Lasslop, G., Law, B. E., Lindroth, A., Merbold, L., Montagnani, L., Moors, E. J., Papale, D., Sottocornola, M., Vaccari, F., and Williams, C: Global patterns of land-atmosphere fluxes of carbon dioxide, latent heat, and sensible heat derived from eddy covariance, satellite, and meteorological observations, J. Geophys. Res., 116, G00J07, doi:10.1029/2010JG001566, 2011.

Liu, J., Fung, I., Kalnay, E., Kang, J. S., Olsen, E. T., and Chen, L.: Simultaneous assimilation of AIRS X_{CO_2} and meteorological observations in a carbon climate model with an ensemble Kalman filter, J. Geophys. Res., 117, D05309, doi:10.1029/2011JD016642, 2012.

Nassar, R., Jones, D. B. A., Kulawik, S. S., Worden, J. R., Bowman, K. W., Andres, R. J., Suntharalingam, P., Chen, J. M., Brenninkmeijer, C. A. M., Schuck, T. J., Conway, T. J., and Worthy, D. E.: Inverse modeling of CO_2 sources and sinks using satellite observations of CO_2 from TES and surface flask measurements, Atmos. Chem. Phys., 11, 6029–6047, doi:10.5194/acp-11-6029-2011, 2011.

Parrish, D. F. and Derber, J. C.: The National Meteorological Center's spectral statistical-interpolation analysis system, Mon. Weather Rev., 120, 1747–1763, 1992.

Rienecker, M. M., Suarez, M. J., Todling, R., Bacmeister, J., Takacs, L., Liu, H.-C., Gu, W., Sienkiewicz, M., Koster, R. D., Gelaro, R., Stajner, I., and Nielsen, J. E.: The GEOS-5 Data Assimilation System-Documentation of versions 5.0.1, 5.1.0, and 5.2.0, NASA Tech. Rep. 104606 V27, 2008.

Rienecker, M. M., Suarez, M. J., Gelaro, R., Todling, R., Bacmeister, J., Liu, E., Bosilovich, M. G., Schubert, S. D., Takacs, L., Kim, G. K., Bloom, S., Chen, J. Y., Collins, D., Conaty, A., Da Silva, A., Gu, W., Joiner, J., Koster, R. D., Lucchesi, R., Molod, A., Owens, T., Pawson, S., Pegion, P., Redder, C. R., Reichle, R., Robertson, F. R., Ruddick, A. G., Sienkiewicz, M., and Woollen, J.: MERRA – NASA's modern-era retrospective analysis for research and applications, J. Climate, 24, 3624–3648, 2011.

Reichle, R. H., Koster, R. D., De Lannoy, G. J. M., Forman, B. A., Liu, Q., Manhanama, S. P. P., and Toure, A.: Assessment and enhancement of MERRA landsurface hydrology estimates, J. Climate, 24, 6322–6338, doi:10.1175/JCLI-D-10-05033.1, 2011.

ACPD
12, 26685–26717, 2012

Singh, H. B., Brune, W. H., Crawford, J. H., Flocke, F., and Jacob, D. J.: Chemistry and transport of pollution over the Gulf of Mexico and the Pacific: spring 2006 INTEX-B campaign overview and first results, Atmos. Chem. Phys., 9, 2301–2318, doi:10.5194/acp-9-2301-2009, 2009.

Stajner, I., Riishöjgaard, L. P., and Rood, R. B.: The GEOS ozone data assimilation system: specification of error statistics, Q. J. Roy. Meteorol. Soc., 127, 1069–1094, 2001.

Stajner, I., Wargan, K., Pawson, S., Hayashi, H., Chang, L. P., Hudman, R. C., Froidevaux, L., Livesey, N., Levelt, P. F., Thompson, A. M., Tarasick, D. W., Stubi, R., Andersen, S. B., Yela, M., Konig-Langlo, G., Schmidlin, F. J., Witte, J. C.: Assimilated ozone from EOS-Aura: evaluation of the tropopause region and tropospheric columns, J. Geophys. Res., 113, D16532, doi:10.1029/2007JD008863, 2008.

Strow, L. L. and Hannon, S. E.: A 4-year zonal climatology of lower tropospheric CO_2 derived from ocean-only Atmospheric Infrared Sounder observations, J. Geophys. Res., 113, D18302, doi:10.1029/2007JD009713, 2008

Tangborn, A., Stajner, I., Buchwitz, M., Khlystova, I., Pawson, S., Hudman, R., and Nedelec, P.: Assimilation of SCIAMACHY total column CO observations; global and regional analysis of data impact, J. Geophys. Res., 114, D07307, doi:10.1029/2008JD010781, 2009.

van der Werf, G. R., Randerson, J. T., Giglio, L., Collatz, G. J., Kasibhatla, P. S., and Arellano Jr., A. F.: Interannual variability in global biomass burning emissions from 1997 to 2004, Atmos. Chem. Phys., 6, 3423–3441, doi:10.5194/acp-6-3423-2006, 2006.

Yokota, T., Yoshida, Y., Eguchi, N., Ota, Y., Tanaka, T., Watanabe, H., and Maksyutov, S.: Global concentrations of CO_2 and CH_4 retrieved from GOSsAT: first preliminary results, SOLA, 5, 160–163, doi:10.2151/sola.2009-041, 2009.

ACPD

12, 26685–26717, 2012

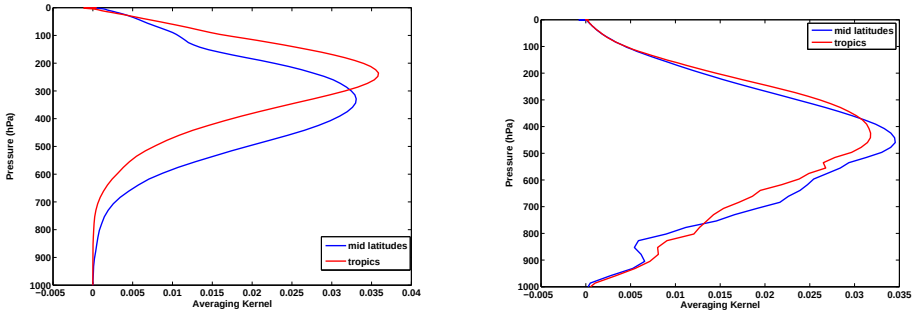

Fig. 1. Typical averaging Kernels for AIRS CO_2 retrieval from **(a)** a set of 15 µm spectral channels (e.g. Chahine et al., 2008), and **(b)** a cluster of channels near the 4 µm waveband.

ACPD
12, 26685–26717, 2012

Evaluation of a new middle-lower tropospheric CO_2 product

A. Tangborn et al.

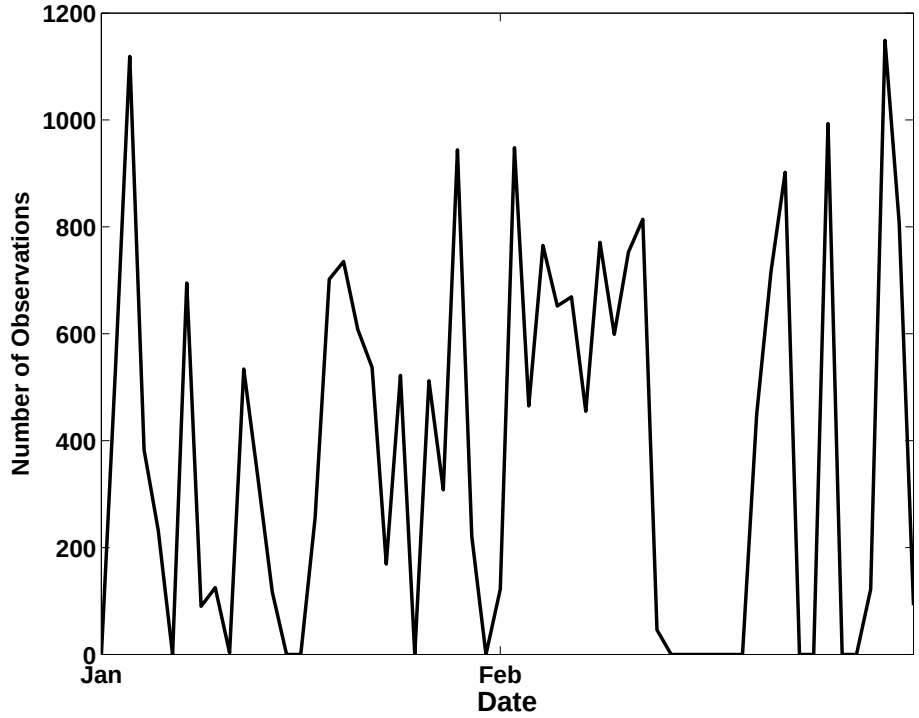

Fig. 2. Daily observation count for clear sky AIRS observations used in the data assimilation system for January/February 2005, superobbed to a 2° × 2.5° grid.

ACPD
12, 26685–26717, 2012

Evaluation of a new middle-lower tropospheric CO_2 product

A. Tangborn et al.

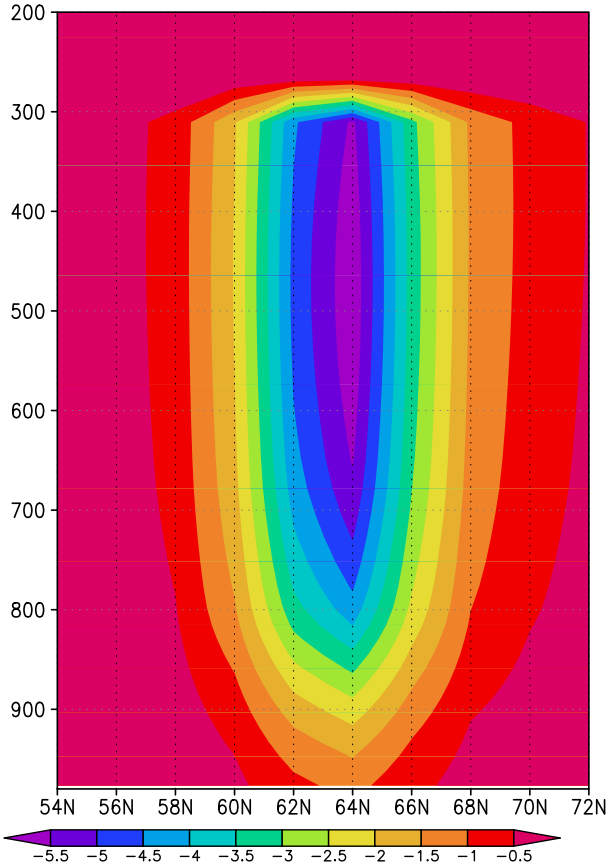

Fig. 3. The latitude-height structure of Analysis increment for CO_2 (ppm) computed in GEOS-5 at 135° W between 54° N and 72° N on 1 July 2006 at 135° W.

ACPD
12, 26685–26717, 2012

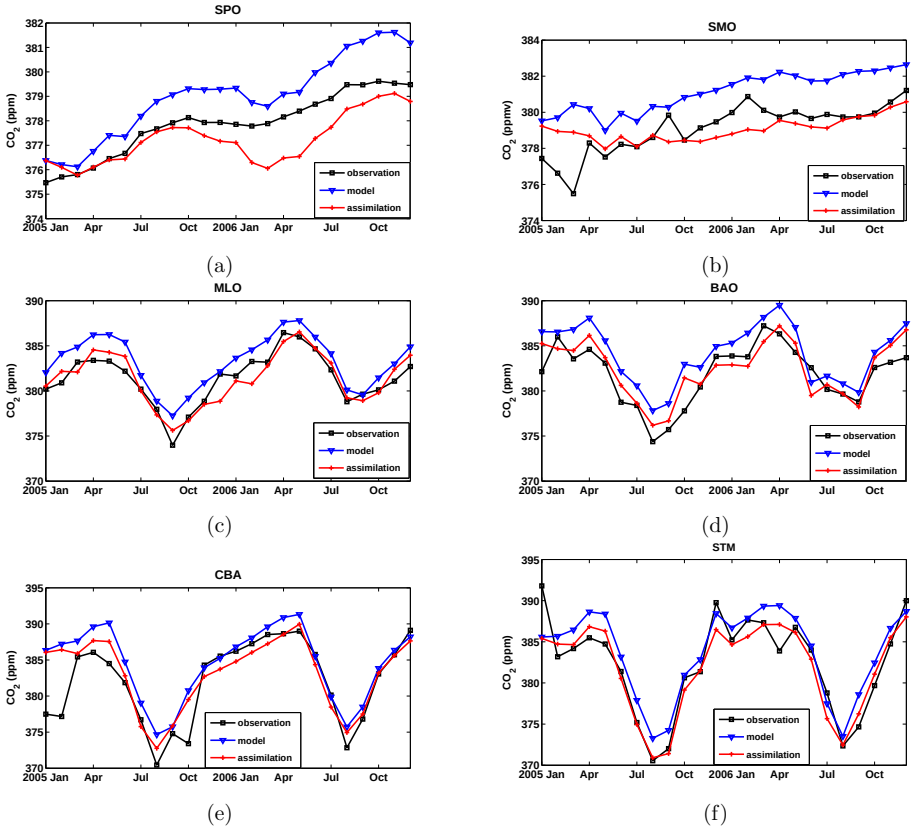

Fig. 4. Monthly mean CO_2 from NOAA/ESRL/GMD cooperative air sampling network (black), GEOS-5 interpolated to the observation locations, for simulations (blue) and with AIRS data assimilated (red). The sites used here are **(a)** SPO (89.96° S, 24.8° W), **(b)** SMO (14.25° S, 170.56° W), **(c)** MLO (19.5° N, 155.6° W), **(d)** BAO (40.0° N, 105.0° W), **(e)** CBA (55.2° N, 162.7° W), **(f)** STM (66° N, 2° N).

ACPD
12, 26685–26717, 2012

Evaluation of a new middle-lower tropospheric CO_2 product

A. Tangborn et al.

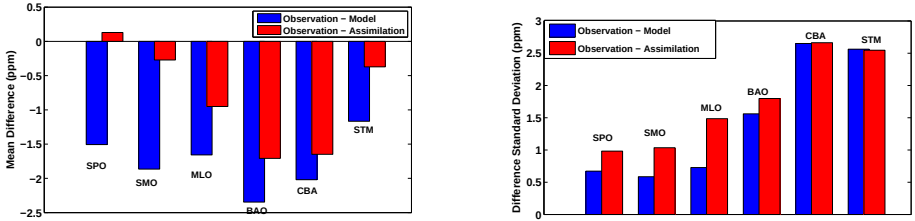

(a) (b)

Fig. 5. Mean **(a)** and standard deviation **(b)** differences ($O - F$) between NOAA/ESRL/GMD cooperative air sampling network and model (blue) or analysis (red) fields interpolated to observation locations. The sites used here are the same as those in Fig. 4, and are ordered from south to north.

ACPD
12, 26685–26717, 2012

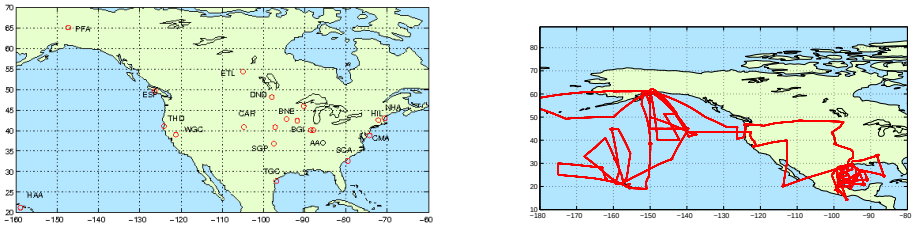

(a) (b)

Fig. 6. Locations of measurements for **(a)** NOAA/ESRL aircraft data and **(b)** INTEX-B flights.

ACPD
12, 26685–26717, 2012

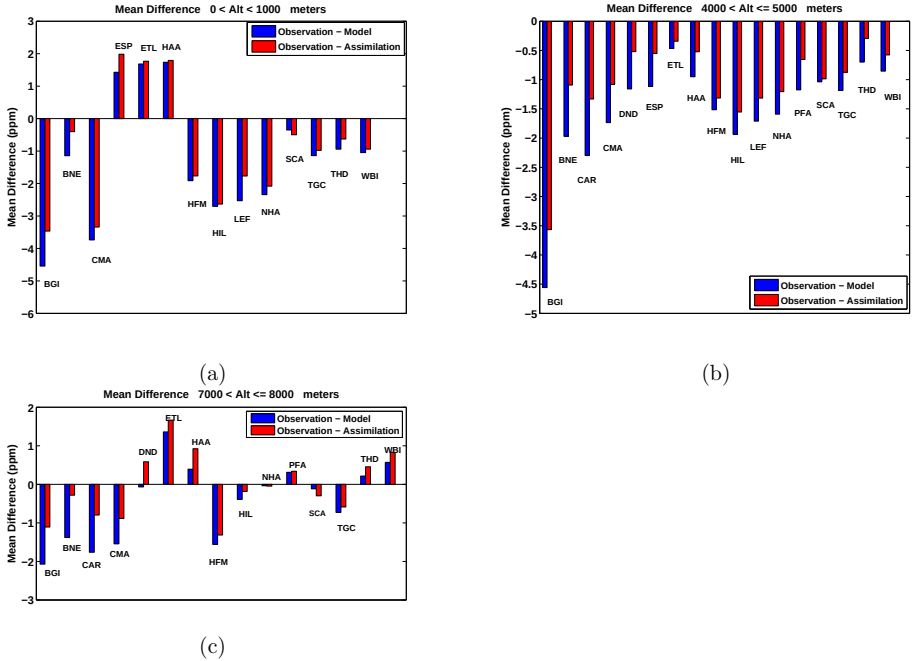

Fig. 7. Mean difference (observation–analysis) between the NOAA/ESRL aircraft data and CO_2 from the GEOS-5 model (or assimilation) interpolated to the observation locations, during the period 1 January 2005–31 December, 2006.

ACPD
12, 26685–26717, 2012

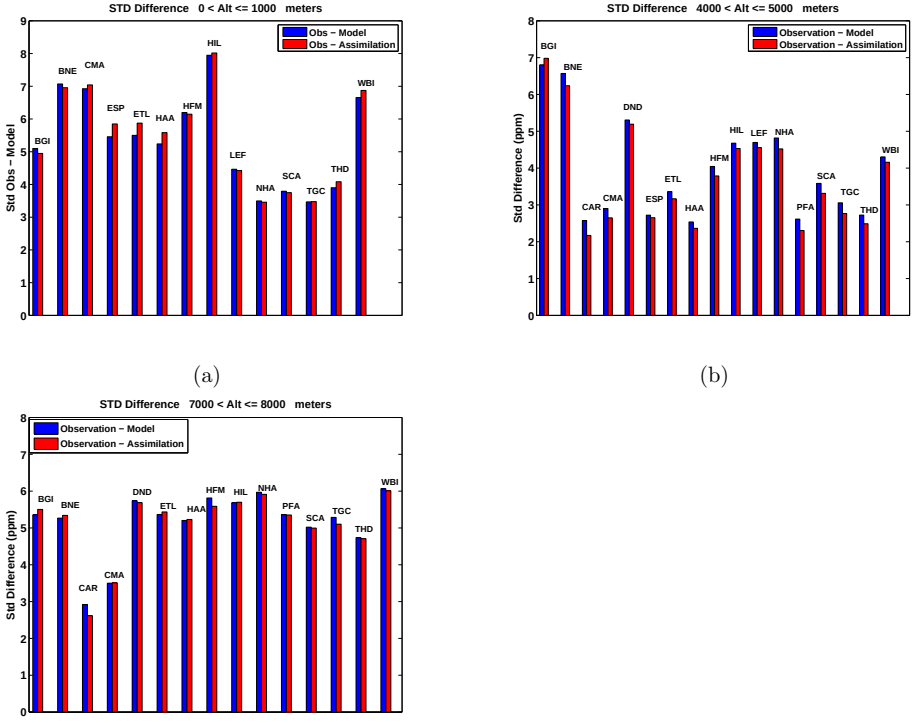

Fig. 8. Standard deviation of difference between the NOAA/ESRL aircraft data and CO_2 from the GEOS-5 model (or assimilation) interpolated to the observation locations, during the period 1 January 2005–31 December, 2006.

ACPD
12, 26685–26717, 2012

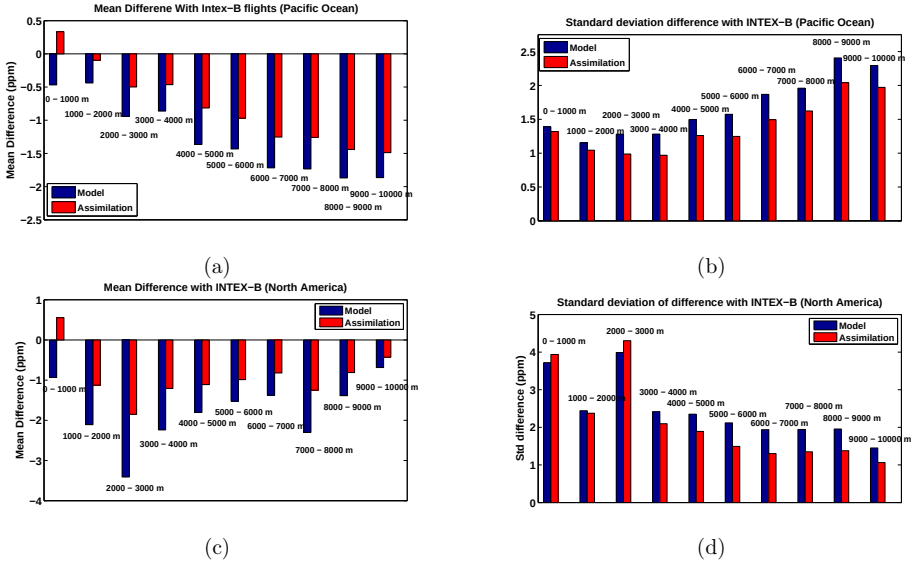

Fig. 9. Mean **(a)** and standard deviation **(b)** of difference (observation–analysis) between the INTEX-B campaign measurements and CO_2 from the GEOS-5 model (or assimilation) interpolated to observation locations over the Pacific Ocean, during the period February–May, 2006. The same plots but with observations restricted to the flights over North America are shown in **(c)** and **(d)**.

ACPD
12, 26685–26717, 2012

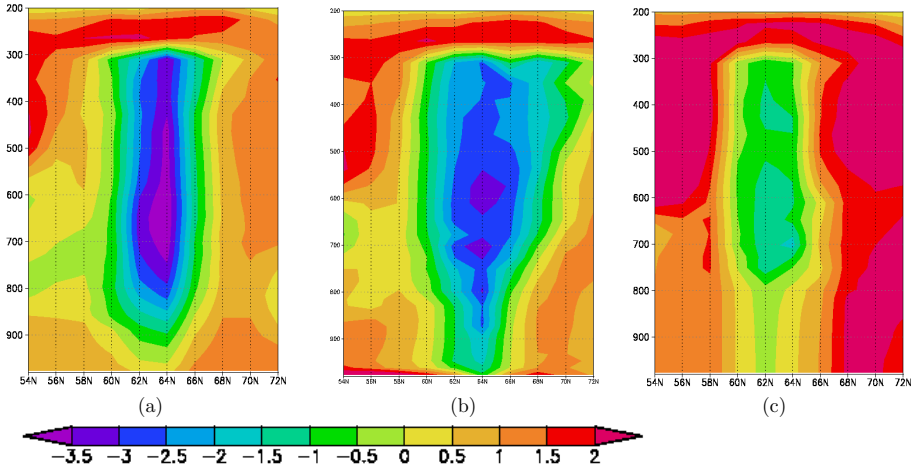

Fig. 10. Cross section of CO_2 differences between the assimilation and the simulation, along latitude lines that follow the local maximum difference on 1 July, 0Z, 135° W **(a)**; 1 July, 12Z, 130° W **(b)** and 1 July, 0Z, 125° W **(c)**.

ACPD
12, 26685–26717, 2012

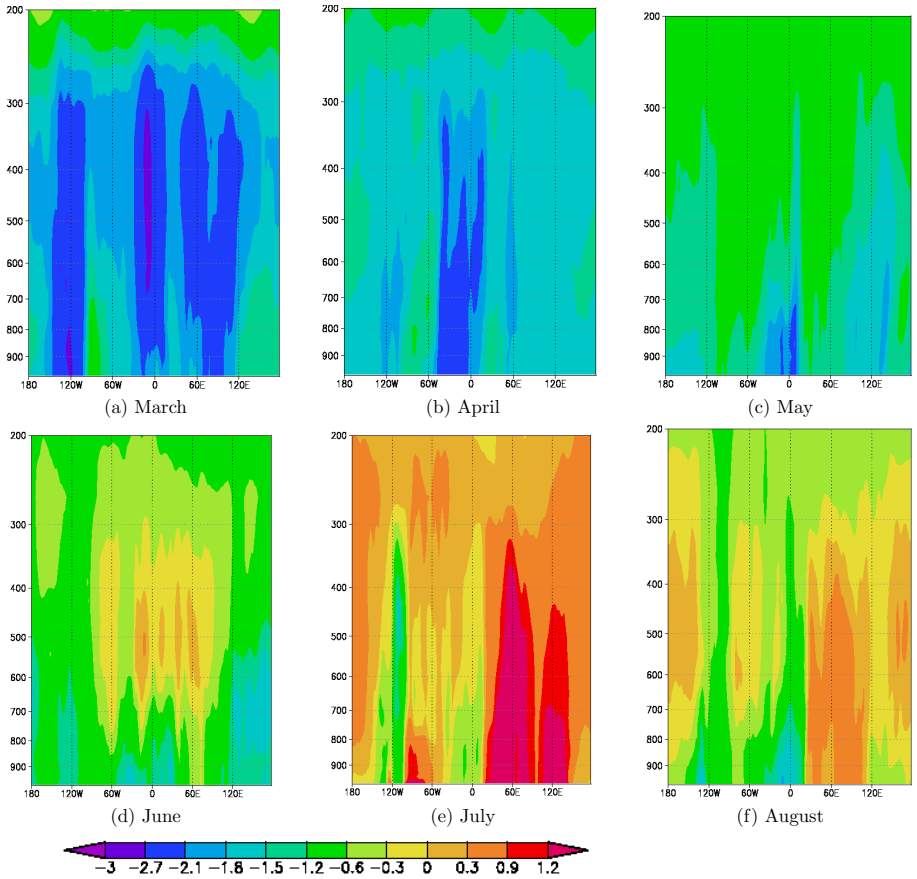

Fig. 11. Monthly mean differences between the assimilation run and free model run at 40° N, for the period March–August, 2005.

ACPD
12, 26685–26717, 2012

Evaluation of a new middle-lower tropospheric CO_2 product

A. Tangborn et al.

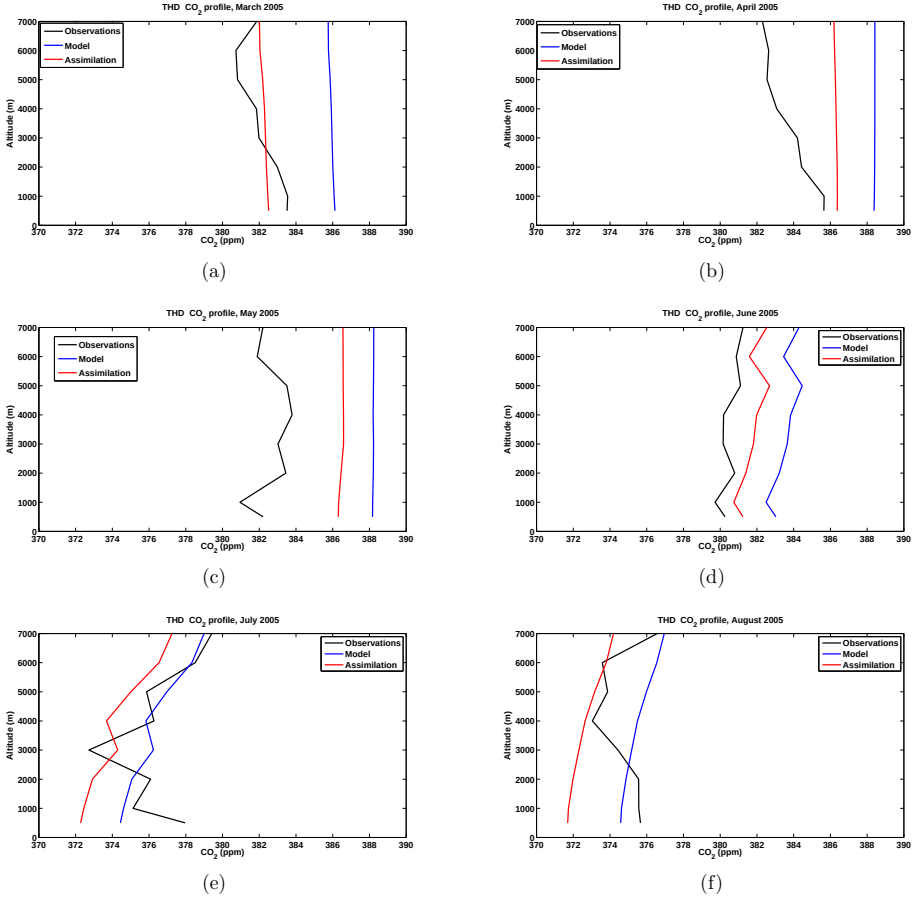

Fig. 12. Monthly mean profiles of CO_2 from CMDL aircraft data (black lines) at the Trinidad Head Observatory (THD, 124° W, 41° N), along with free running model (blue) and assimilation (red) output interpolated to the aircraft measurement locations, for the period March–August 2005.

ACPD
12, 26685–26717, 2012

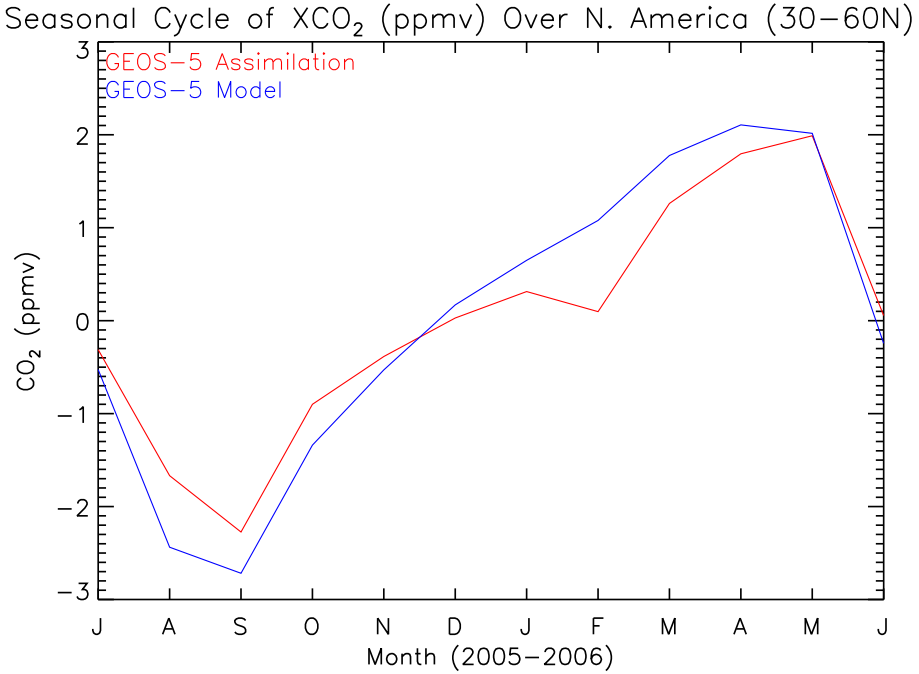

Fig. 13. Seasonal cycle of column-averaged CO_2 mixing ratio (ppmv) for the assimilation (red) and model (blue) calculated by detrending time series of monthly mean CO_2 over North America and then calculating departure from the annual (July 2005 through June 2006) mean.

ACPD
12, 26685–26717, 2012